Electronic Supplementary Material (ESI) for Materials Advances.

SUPPLEMENTARY INFORMATION

Delving into the Multifunctionality of $Sr_2NaMg_2V_3O_{12}$ *via* RE^{3+} Substitution for Dual-mode Temperature Sensing, Latent Fingerprint Detection, and Security Inks

Amrithakrishnan Bindhu[a], Jawahar Isuhak Naseemabeevi[a], Subodh Ganesanpotti[a] *

[a]Department of Physics, University of Kerala, Kariavattom Campus, Thiruvananthapuram, Kerala - 695 581, India

Email: gsubodh@gmail.com, gsubodh@keralauniversity.ac.in

Table S1 Rietveld refinement and crystallographic parameters of $Sr_{1.9}Sm_{0.05}Na_{1.05}Mg_2V_3O_{12}$.

Formula		$Sr_{1.9}Sm_{0.05}Na_{1.05}Mg_2V_3O_{12}$				
Crystal system		Cubic				
Space group		$Ia\bar{3}d$ (230, O_h^{10})				
Cell parameter		a=12.652(1) Å				
Reliability factors		R_{wp}= 5.35%, R_p= 4.07% and GOF= 1.19				
Atom	Site	x	y	z	Occupancy	B_{eq} (Å^2)
Sr^{2+}/Sm^{3+}	24c	0.375	0.5	0.25	0.667	0.009(5)
Na^+	24c	0.375	0.5	0.25	0.333	0.009(5)
Mg^{2+}	16a	0.50	0.5	0	1	0.008(1)
V^{5+}	24d	0.625	0.50	0.25	1	0.005(8)
O^{2-}	96h	0.039(8)	0.048(9)	0.653(6)	1	0.009(6)

Table S2 Rietveld refinement and crystallographic parameters of $Sr_{1.76}Sm_{0.12}Na_{1.12}Mg_2V_3O_{12}$.

Formula		$Sr_{1.76}Sm_{0.12}Na_{1.12}Mg_2V_3O_{12}$				
Crystal system		Cubic				
Space group		$Ia\bar{3}d$ (230, O_h^{10})				
Cell parameter		a=12.644(8) Å				
Reliability factors		R_{wp}= 5.28%, R_p= 3.95 % and GOF= 1.25				
Atom	Site	x	y	z	Occupancy	B_{eq} (Å^2)
Sr^{2+}/Sm^{3+}	24c	0.375	0.5	0.25	0.667	0.009(8)
Na^+	24c	0.375	0.5	0.25	0.333	0.009(8)
Mg^{2+}	16a	0.50	0.5	0	1	0.007(9)
V^{5+}	24d	0.625	0.50	0.25	1	0.006(1)
O^{2-}	96h	0.039(8)	0.045(9)	0.652(3)	1	0.009(8)

Table S3 Raman band assignment of Sm^{3+} activated SNMV system.

Band/ type of motion	Irreducible representation	Ω (cm^{-1})	γ (cm^{-1})
T of Sr/NaO_8	F_{2g}	105	8
T of VO_4	E_g	146	13
R of VO_4	E_g	215	5
R of VO_4	A_{1g}	256	24
υ_2	A_{1g}	332	15
υ_4	F_{2g}	366	30
υ_2	E_g	447	22
υ_3	F_{2g}	758	46
υ_1	A_{1g}	834	25
υ_4	E_g	891	7
υ_1	E_g	912	21
υ_3	F_{2g}	1229	29
υ_3	E_g	1366	31
υ_3	F_{2g}	1451	27
υ_3	F_{2g}	1506	87

Table S4. The variation of CIE coordinates with Sm^{3+} concentration.

Sm^{3+} concentration	CIE coordinates
0.01	(0.202, 0.286)
0.03	(0.218, 0.291)
0.05	(0.234, 0.298)
0.07	(0.238, 0.299)
0.10	(0.248, 0.303)
0.12	(0.265, 0.315)

Table S5 List of thermographic phosphors reported for thermochromic luminescence.

Compounds	Temperature range (K)	CIE shift	Reference
$Ba_3(VO_4)_2$: Sm^{3+}	303-463	(0.310, 0.412) to (0.375, 0.338) Green to White	1
$LiCa_3ZnV_3O_{12}$: Sm^{3+}	303- 463	(0.364, 0.388) to (0.569, 0.391) White to red	2
$Na_3Sc_2P_3O_{12}$: Eu^{2+}/ Mn^{2+}	293 -473	(0.468, 0.308) to (0.315, 0.231) Red to purple	3
$BaGd_2O_4$: Bi^{3+}/Sm^{3+}	293-473	(0.2584, 0.1765) to (0.3373, 0.2581) Lavender to pink	4
$LaNbO_4$: Bi^{3+}/Eu^{3+}	303-483	(0.3695, 0.2707) to (0.5822, 0.3418)	5
$LaNbO_4$: Bi^{3+}/Tb^{3+}	303-483	(0.2197, 0.2427) to (0.3151, 0.4526)	5

$Lu_3Al_5O_{12}$: Ce^{3+}/Mn^{4+}	298-353	(0.4525, 0.4673) to (0.3665, 0.5247) Red to green	6
$Ca_2NaMg_2V_3O_{12}$: Eu^{3+}	303-503	Green to reddish orange	7
$Ca_2NaMg_2V_3O_{12}$: Sm^{3+}	303-503	Green to orange	7
$Ca_2NaZn_2V_3O_{12}$: Eu^{3+}	303-483	(0.421, 0.396) to (0.629, 0.350) Yellowish red to pure red	8
$Sr_2NaMg_2V_3O_{12}$: Eu^{3+}	300-500	(0.353, 0.335) to (0.611, 0.360) White to deep red	9
$Sr_2NaMg_2V_3O_{12}$: Sm^{3+}	300-500	(0.263, 0.352) (0.504, 0.408) Cyan to orange-red	This work

Table S6 Rietveld refinement and crystallographic parameters of $Sr_{1.7}Eu_{0.15}Na_{1.15}Mg_2V_3O_{12}$.

Formula	$Sr_{1.7}Eu_{0.15}Na_{1.15}Mg_2V_3O_{12}$					
Crystal system	Cubic					
Space group	$Ia\bar{3}d$ (230, O_h^{10})					
Cell parameter	a=12.624(5) Å					
Reliability factors	R_{wp}= 3.07%, R_p= 2.37% and GOF= 1.38					
Atom	Site	x	y	z	Occupancy	B_{eq} (Å^2)
Sr^{2+}/Eu^{3+}	24c	0.375	0.5	0.25	0.667	0.009(5)
Na^+	24c	0.375	0.5	0.25	0.333	0.009(5)
Mg^{2+}	16a	0.50	0.50	0	1	0.008(1)
V^{5+}	24d	0.625	0.50	0.25	1	0.005(8)
O^{2-}	96h	0.039(7)	0.049(2)	0.653(7)	1	0.009(6)

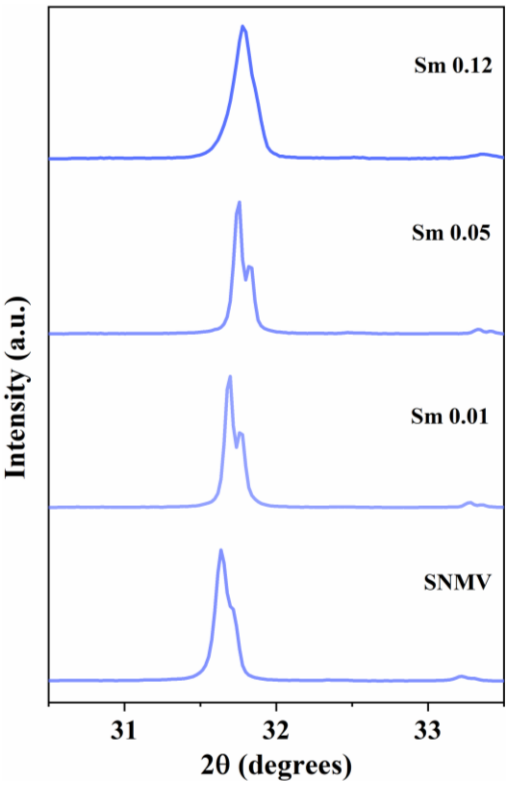

Figure S1: The shift of Bragg peak with Sm^{3+} concentration.

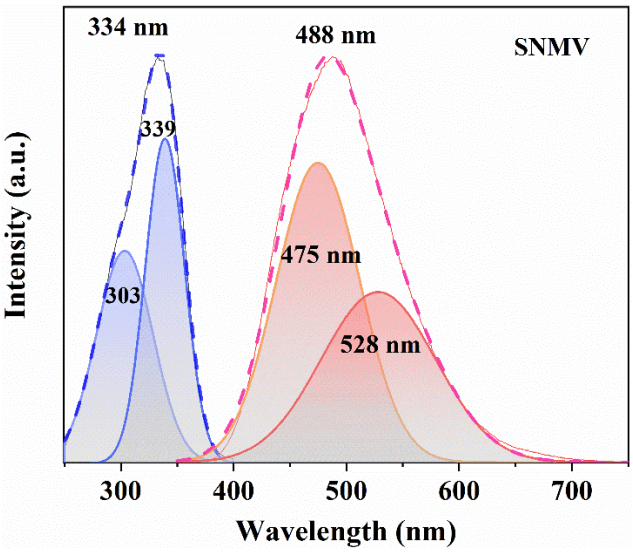

Figure S2. The photoluminescence emission and excitation spectra of SNMV phosphor.

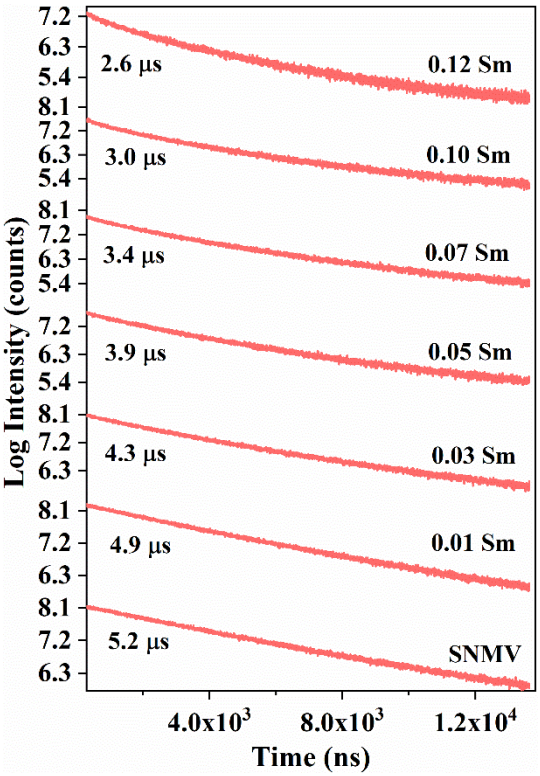

Figure S3. The luminescence dependent decay time with Sm^{3+} concentration.

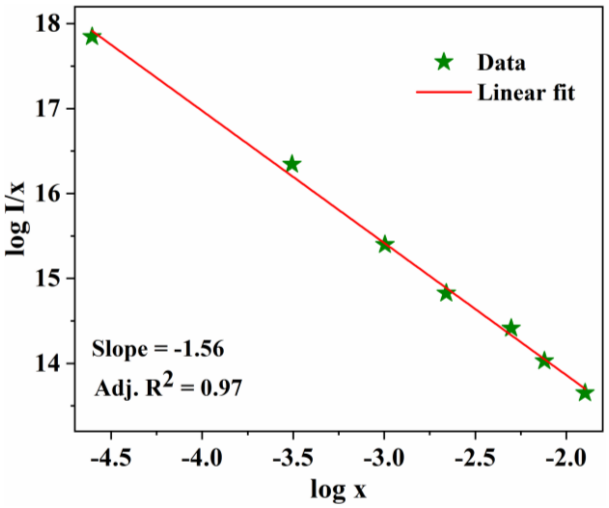

Figure S4 Plot of *ln (I/x)* vs. *ln x* of SNMV: Sm^{3+} at various concentrations.

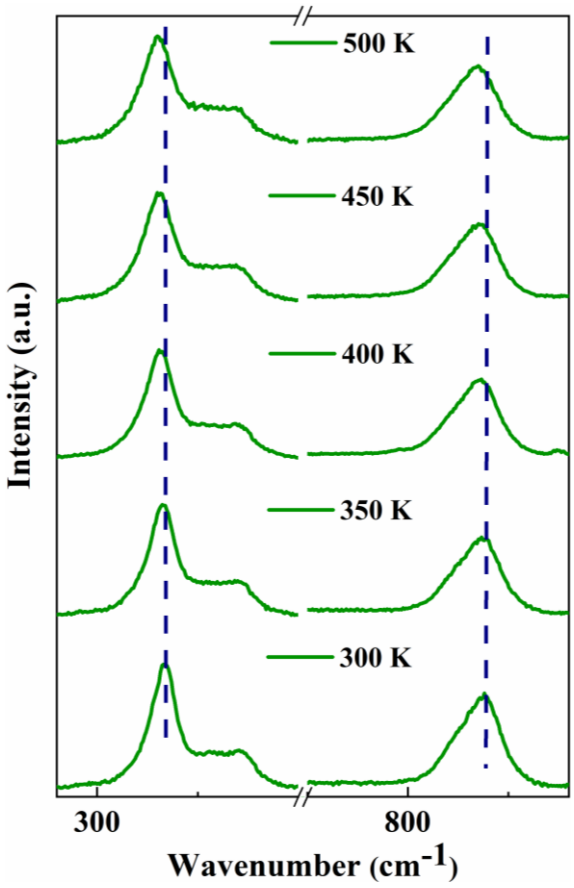

Figure S5 Temperature-dependent Raman spectra of SNMV: 0.05 Sm^{3+} phosphor.

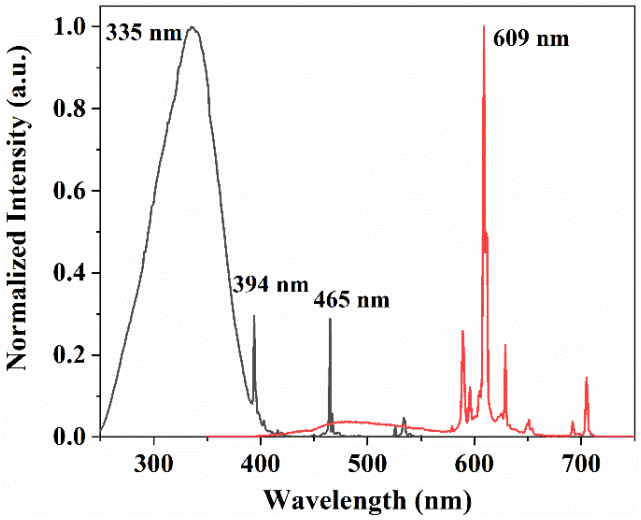

Figure S6. The photoluminescence emission and excitation spectra of SNMV: 0.15 Eu^{3+} phosphor.

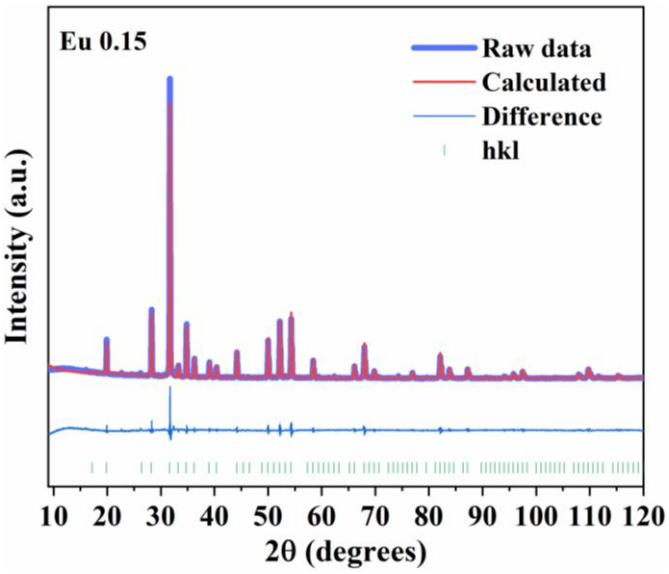

Figure S7 Rietveld refinement pattern of SNMV: 0.15 Eu^{3+}.

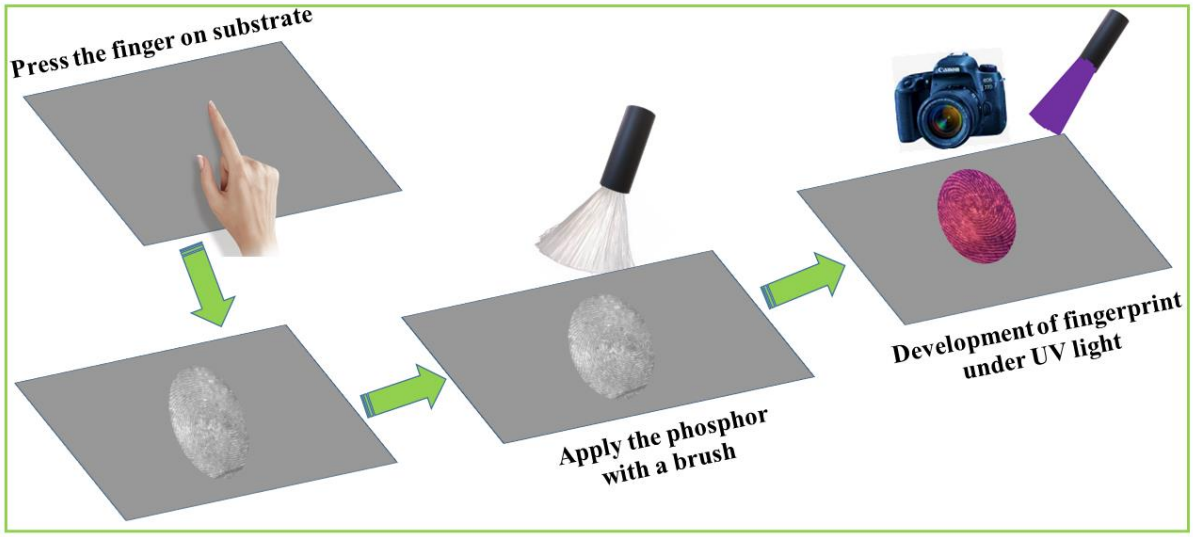

Figure S8 Schematic illustration of latent fingerprint detection.

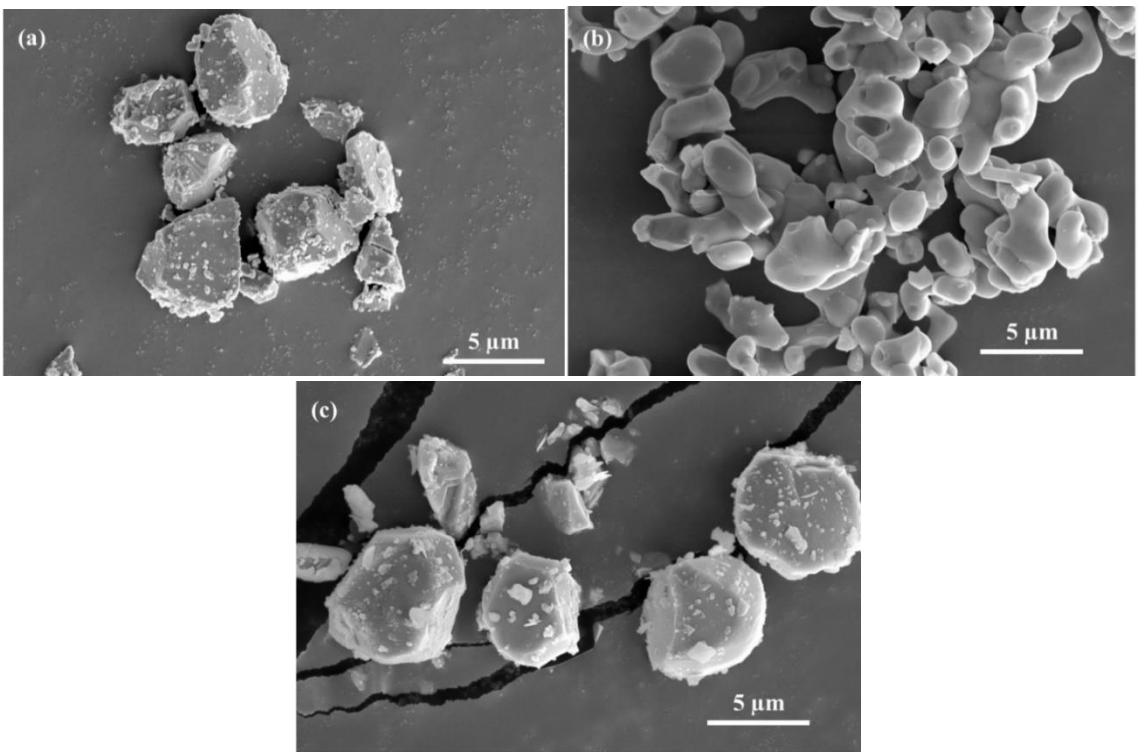

Figure S9 FE-SEM images of (a) SNMV: 0.15 Eu^{3+}, (b) SNMV, and (c) SNMV: 0.05 Sm^{3+} phosphors.

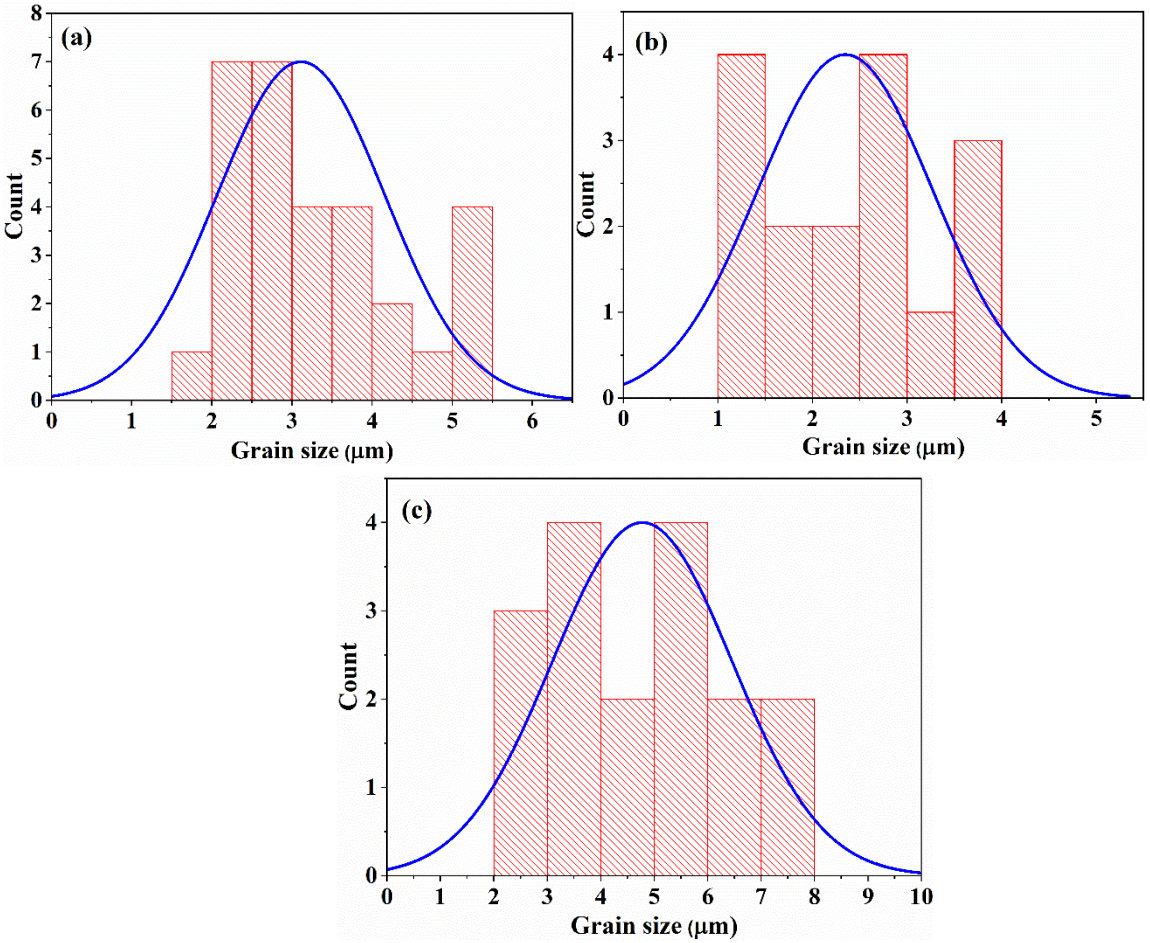

Figure S10 Grain size distribution in (a) SNMV: 0.15 Eu^{3+}, (b) SNMV, and (c) SNMV: 0.05 Sm^{3+}.

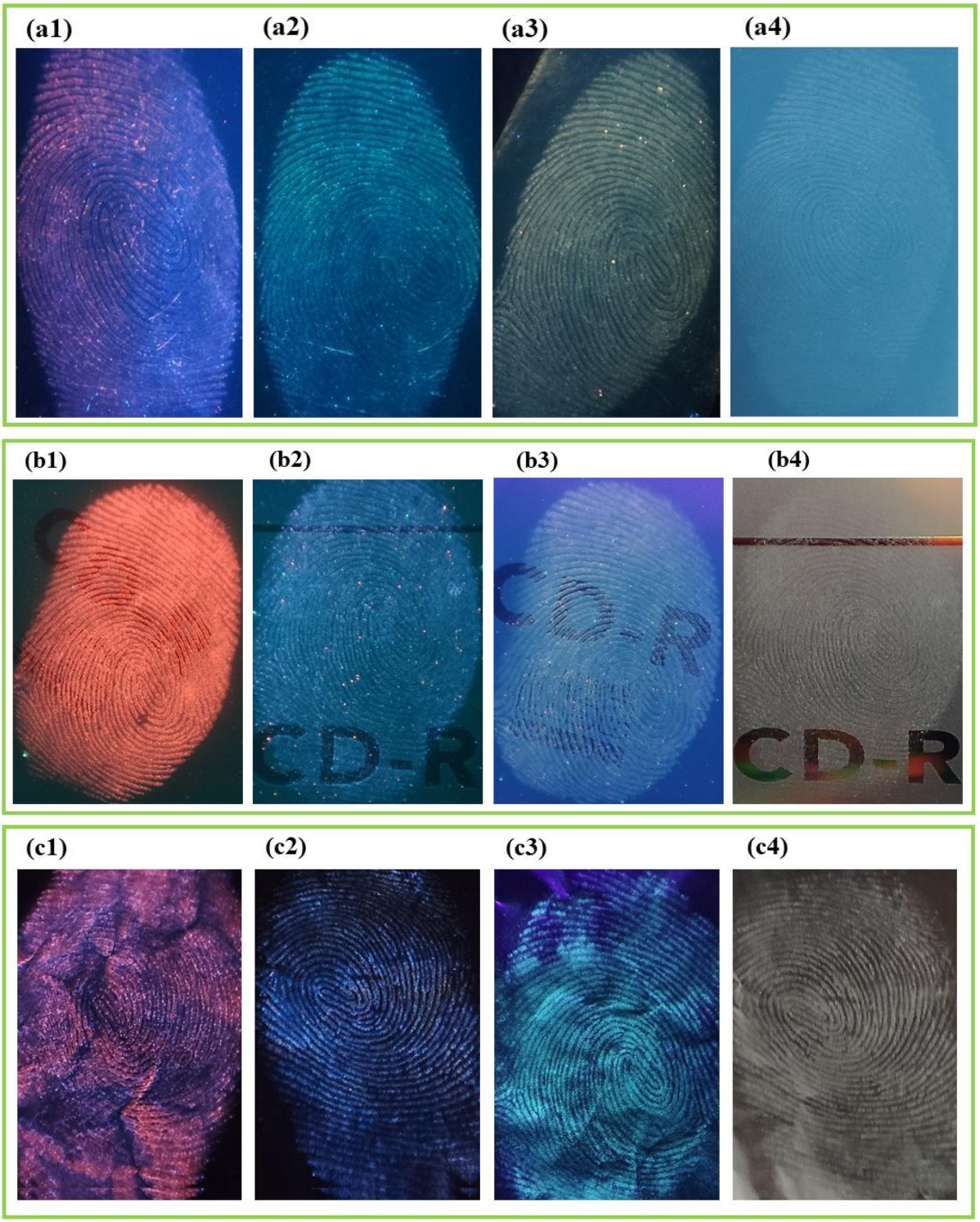

Figure S11 The digital photographs of LFPs illuminated on various substrates- (a1-a3) highlighter, (b1-b3) CD and (c1-c3) under UV radiation of 365 nm using (1) SNMV: Eu^{3+}, (2) SNMV, (3) SNMV: Sm^{3+} phosphors and (4) under daylight respectively.

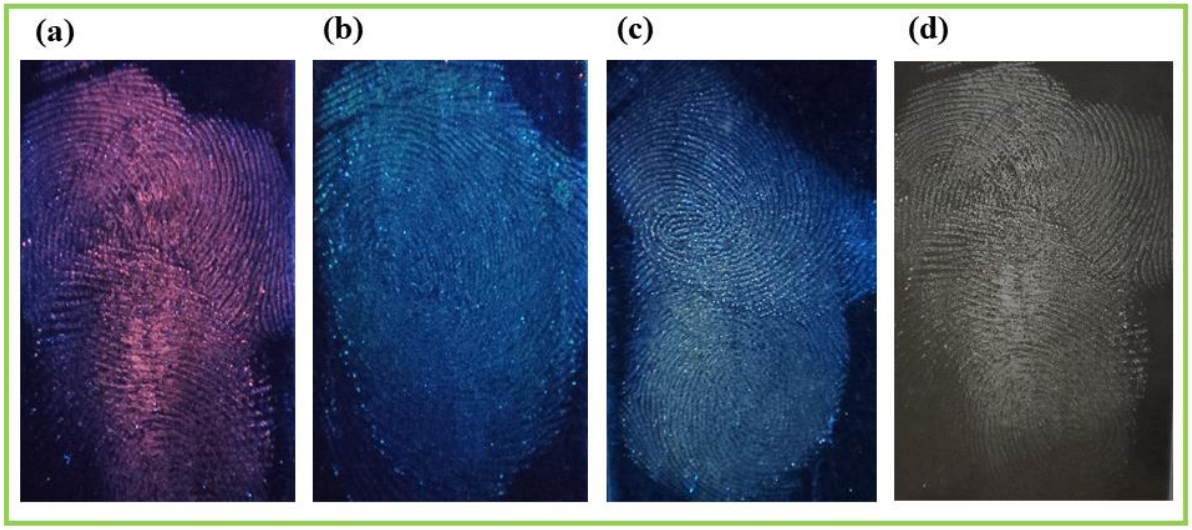

Figure S12 Visualization of smudged LFPs based on (a) SNMV: Eu^{3+}, (b) SNMV, (c) SNMV: Sm^{3+} based LFPs on the glass slide under UV radiation of 365 nm and (d) under daylight.

References

(1) Du, P.; Hua, Y.; Yu, J. S. Energy Transfer from VO_4^{3-} Group to Sm^{3+} Ions in $Ba_3(VO_4)_2$:3xSm^{3+} Microparticles: A Bifunctional Platform for Simultaneous Optical Thermometer and Safety Sign. *Chemical Engineering Journal* **2018**, *352*, 352–359. https://doi.org/10.1016/J.CEJ.2018.07.019

(2) Guo, H.; Devakumar, B.; Vijayakumar, R.; Du, P.; Huang, X. A Novel Sm^{3+} Singly Doped $LiCa_3ZnV_3O_{12}$ Phosphor: A Potential Luminescent Material for Multifunctional Applications. *RSC Adv* **2018**, *8* (58), 33403–33413. https://doi.org/10.1039/C8RA07329E

(3) Zhang, X.; Zhu, Z.; Guo, Z.; Sun, Z.; Chen, Y. A Ratiometric Optical Thermometer with High Sensitivity and Superior Signal Discriminability Based on $Na_3Sc_2P_3O_{12}$: Eu^{2+}, Mn^{2+}

Thermochromic Phosphor. *Chemical Engineering Journal* **2019**, *356*, 413–422. https://doi.org/10.1016/J.CEJ.2018.09.075

(4) Fu, J.; Zhou, L.; Chen, Y.; Lin, J.; Ye, R.; Deng, D.; Chen, L.; Xu, S. Dual-Mode Optical Thermometry Based on Bi^{3+}/Sm^{3+} Co-Activated $BaGd_2O_4$ Phosphor with Tunable Sensitivity. *J Alloys Compd* **2022**, *897*, 163034. https://doi.org/10.1016/J.JALLCOM.2021.163034

(5) Xue, J.; Yu, Z.; Noh, H. M.; Lee, B. R.; Choi, B. C.; Park, S. H.; Jeong, J. H.; Du, P.; Song, M. Designing Multi-Mode Optical Thermometers via the Thermochromic $LaNbO_4:Bi^{3+}/Ln^{3+}$ (Ln = Eu, Tb, Dy, Sm) Phosphors. *Chemical Engineering Journal* **2021**, *415*, 128977. https://doi.org/10.1016/J.CEJ.2021.128977

(6) Chen, Y.; He, J.; Zhang, X.; Rong, M.; Xia, Z.; Wang, J.; Liu, Z. Q. Dual-Mode Optical Thermometry Design in $Lu_3Al_5O_{12}:Ce^{3+}/Mn^{4+}$ Phosphor. *Inorg Chem* **2020**, *59* (2), 1383–1392. https://doi.org/10.1021/ACS.INORGCHEM.9B03107

(7) Zhou, H.; Guo, N.; Lü, X.; Ding, Y.; Wang, L.; Ouyang, R.; Shao, B. Ratiometric and Colorimetric Fluorescence Temperature Sensing Properties of Trivalent Europium or Samarium Doped Self-Activated Vanadate Dual Emitting Phosphors. *J Lumin* **2020**, *217*, 116758. https://doi.org/10.1016/J.JLUMIN.2019.116758

(8) Du, P.; Yu, J. S. Self-Activated Multicolor Emissions in $Ca_2NaZn_2(VO_4)_3:Eu^{3+}$ Phosphors for Simultaneous Warm White Light-Emitting Diodes and Safety Sign. *Dyes and Pigments* **2017**, *147*, 16–23. https://doi.org/10.1016/J.DYEPIG.2017.07.065

(9) Bindhu, A.; Naseemabeevi, J. I.; Ganesanpotti, S. Vibrationally Induced Photophysical Response of $Sr_2NaMg_2V_3O_{12}:Eu^{3+}$ for Dual-Mode Temperature Sensing and Safety Signs. *Adv Photonics Res* **2022**, *3* (6), 2100159. https://doi.org/10.1002/ADPR.202100159